Porous silicon membrane-modified electrodes for label-free voltammetric detection of MS2 bacteriophage

Nekane Reta, Andrew Michelmore, Christopher Saint, Beatriz Prieto-Simón, Nicolas H. Voelcker

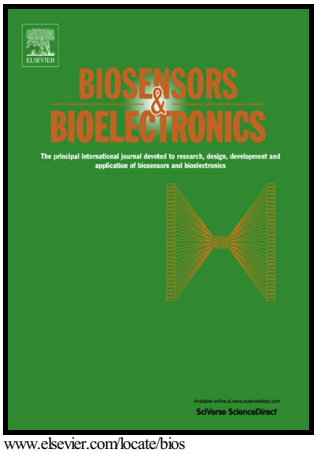

www.elsevier.com/locate/bios

PII: S0956-5663(16)30037-9
DOI: http://dx.doi.org/10.1016/j.bios.2016.01.038
Reference: BIOS8378

To appear in: *Biosensors and Bioelectronic*

Received date: 5 November 2015
Revised date: 12 January 2016
Accepted date: 13 January 2016

Cite this article as: Nekane Reta, Andrew Michelmore, Christopher Saint, Beatri Prieto-Simón and Nicolas H. Voelcker, Porous silicon membrane-modifie electrodes for label-free voltammetric detection of MS2 bacteriophag *Biosensors and Bioelectronic,* http://dx.doi.org/10.1016/j.bios.2016.01.038

Porous silicon membrane-modified electrodes for label-free voltammetric detection of MS2 bacteriophage

Nekane Reta, [a] Andrew Michelmore, [a,b] Christopher Saint, [c] Beatriz Prieto-Simón,[*, a] and Nicolas H. Voelcker[*, a]

[a] *Future Industries Institute, Mawson Lakes, South Australia 5095, Australia*

[b] *School of Advanced Manufacturing and Mechanical Engineering, University of South Australia, Mawson Lakes, South Australia 5095, Australia*

[c] *Centre for Water Management and Re-use, School of Natural & Built Environments, University of South Australia, Mawson Lakes, South Australia 5001, Australia*

Corresponding authors: Prof. Nicolas H. Voelcker, Dr. Beatriz Prieto-Simon

GPO Box 2471, Adelaide, South Australia 5001, Australia

tel: +61 8 8302 5508, fax; +61 8 8302 5613

email: nico.voelcker@unisa.edu.au

beatriz.prietosimon@unisa.edu.au

Abstract

A proof of concept for the label-free detection of bacteriophage MS2, a model indicator of microbiological contamination, is validated in this work as a porous silicon (pSi) membrane-based electrochemical biosensor. PSi membranes were used to afford nanochannel architectures. The sensing mechanism was based on the nanochannel blockage caused by MS2 binding to immobilized capture antibodies. This blockage was quantified by measuring the oxidation current of the electroactive species reaching the electrode surface, by means of

differential pulse voltammetry (DPV). The immunosensor showed a limit of detection of 6 pfu/mL in buffer, allowing the detection of MS2 to levels commonly found in real-world applications, and proved to be unaffected by matrix effects when analyzing MS2 in river water. By choosing the proper functionalization strategy and nanochannels diameter, this platform affords the possibility to simply, directly and sensitively detect a broad range of target analytes, being a promising approach towards the development of point-of-care portable electronic devices.

Keywords: Porous silicon, label free, electrochemical immunoassay, nanochannel blockage, MS2 bacteriophage

1. Introduction

PSi is a promising material for sensing applications due to its tuneable morphology (pore size and porosity), large surface area (up to 800 m^2/g) and versatile chemistry (Harraz 2014; Jane et al. 2009). All these attributes, added to its remarkable optical properties, have motivated cohorts of researchers to pursue the development of pSi-based optical biosensors over the past 15 years (Acquaroli et al. 2014; Bonanno et al. 2010; Dancil et al. 1999; Holthausen et al. 2012; Jenie et al. 2014; Kilian et al. 2007; Krismastuti et al. 2014; Orosco et al. 2006; Sciacca et al. 2011; Szili et al. 2011; Urmann et al. 2015; Voelcker et al. 2008). However, the use of pSi in the design of electrochemical biosensors has arguably been neglected.

Electrochemical biosensors provide an attractive means to detect target molecules due to their sensitivity, selectivity, stability and robustness at a low cost (Bakker 2004; Grieshaber et al. 2008). Moreover, by combining the proper sensing mechanism and detection technique, electrochemical biosensors can be designed to provide label-free detection, which presents shorter analysis time and simplicity over labelled strategies (Vestergaard et al. 2007). Another important advantage is their capability to be miniaturized and thus their potential portability for in-situ analyses. These characteristics, combined with the unique properties of nanostructured materials, are essential for the development of novel biosensing platforms with improved analytical performance in terms of higher sensitivity, selectivity and detection efficiency for real applications (Campas et al. 2012; Yogeswaran and Kumar). Particularly interesting is the use of porous nanostructured materials, featuring arrays of nanochannels. These sensing platforms offer several advantages. The large specific area of these materials is expected to enhance the sensitivity of the device (compared to flat electrodes) due to the increase in the number of immobilized bioreceptors and thus available binding sites (de la Escosura-Muñiz and Merkoçi 2012). Additionally, they are conducive to

a sensing strategy based on nanochannel blockage as a label-free and direct method of measuring the interaction of the analyte and the capture probe immobilized in the channels. The nanochannel blockage impedes the diffusion of any redox probe added in solution to the transducer surface, what can be electrochemically measured. The possibility to engineer molecular recognition capabilities by just tuning the morphology of the nanochannels combined with this label-free strategy offer a simple and rapid method of detection that could be easily adapted to point-of-care devices. Furthermore, the pore volume and size of nanoporous materials can be controlled in a precise way to facilitate their use as membrane filters of interfering compounds, consequently minimizing matrix effects. Among these porous nanostructed materials, nanoporous anodic alumina (NAA) and pSi are promising materials to design high-performing electrochemical platforms for portable testing devices. NAA membranes integrated onto different transducers have been widely used to develop platforms based on nanochannel blockage sensing combined with voltammetric or impedimetric techniques (Cheng et al. 2011; de la Escosura-Muñiz et al. 2013; de la Escosura-Muniz and Mekoci 2010; de la Escosura-Muñiz and Merkoçi 2010, 2011; Kant et al. 2014; Koh et al. 2007; Nguyen et al. 2009; Nguyen et al. 2012; Peh and Li 2013; Rai et al. 2012a; Rai et al. 2012b) (Table S1 in Supplementary data). PSi substrates (pSi films attached to the silicon) have been used to developed electrochemical biosensors, mainly exploiting the large surface area provided (Archer et al. 2004; Archer and Fauchet 2003; Lugo et al. 2007; Reddy et al. 2003; Song et al. 2007; Vamvakaki and Chaniotakis 2008; Zhang et al. 2012), while pSi membrane-modified transducers relying on nanochannel blockage to transduce analyte binding have not been reported yet.

In this context, we present a system based on a pSi membrane to detect MS2 bacteriophage. This bacteriophage was chosen as an indicator of microbiological contamination in water supplies due to its specificity for a target bacterial species, and

robustness compared to bacterial indicators (Brehant et al. 2010). MS2 bacteriophage is ubiquitous in *Escherichia coli* contaminated environments such as wastewater (10^1–10^4 pfu/ml) and raw sewage impacted wetland (30 pfu/ml) and it has been demonstrated that its presence is proportional to the level of faecal contamination (Keegan et al. 2009; Li et al. 2012).

Here, we describe for the first time, a pSi membrane-based immunosensor that exploits nanochannel blockage as the sensing mechanism to detect MS2 bacteriophage. MS2 bacteriophage binding to the immobilized capture antibodies in the nanochannels causes partial blockage of the channels and therefore, impedes the diffusion of the redox probe added in solution to the transducer surface. This causes a decrease in the oxidation current, which is measured using DPV. Our results demonstrate the sensitive detection of MS2 bacteriophage at levels encountered in real situations such as waste water and sewage impacted environments. The simplicity and excellent analytical performance of this proof of concept pave the way towards the development of future label-free electrochemical immunosensors not limited to water analysis but also relevant to food quality testing and biomedical diagnostics.

2. Experimental

2.1. Reagents

N-type silicon wafers with 0.008-0.02 Ωcm resistivity, phosphor doped, (100)-oriented were purchased from Siltronix (France).

Potassium ferrocyanide ($K_4[Fe(CN)_6]$), potassium ferricyanide ($K_3[Fe(CN)_6]$), undecylenic acid, N-hydroxysuccinimide (NHS), N-(3-dimethylaminopropyl) N′-

ethylcarbodiimide hydrochloride (EDC), ethanolamine, phosphate buffered saline (PBS) tablets and 2-(N-morpholino)-ethanesulfonic acid (MES) were purchased from Sigma-Aldrich (Australia). Hydrofluoric acid (HF) (48%, AR grade) was purchased from Scharlau (Australia). Sodium hydroxide (NaOH) (AR grade) was purchased from Merck (Australia) and NCW-1001 surfactant was purchased from Wako Pure Chemical Industries (Japan).

Monoclonal antibody (produced in mouse) against MS2 bacteriophage was purchased from Galahad Sales (TC-7033-001, Australia). Anti-BSA antibody (control) was purchased from Life Technologies (A11133, Australia). MS2 bacteriophage was kindly supplied by the Australian Water Quality Centre, SAWater Corporation. All dilutions were prepared in Milli-Q water.

Gold-coated microscope slides, consisting of 150 nm of gold coating on 10 nm chromium coating, were purchased from Telic Company (USA).

2.2. Apparatus

Electrochemical anodization of silicon was performed using a Keithley (Model 2425, USA) source meter.

Scanning Electron Microscopy (SEM) images were obtained on a FEI QuantaTM 450 Field Emission Gun Environmental Scanning Electron Microscope.

Fourier transform infrared (FT-IR) spectroscopy was performed with a Bruker Hyperion 100 microscope (Bruker Optics, Germany) coupled to a liquid nitrogen cooled Mercury-cadmium-tellurite detector, in reflectance mode. All spectra were taken over the range of 650-4000 cm^{-1} at 4 cm^{-1} resolution, after averaging 64 scans. Background spectra were performed by using a gold coated glass slide.

Electrochemical measurements were carried out on an electrochemical analyzer (CH Instruments, model 600D series, USA) using a three-electrode Teflon cell containing the pSi membrane on gold as the working electrode, silver/silver chloride reference electrode (CH Instruments, USA) and a platinum wire counter electrode (CH Instruments, USA).

2.3. Preparation of pSi membrane

pSi membranes were prepared by electrochemical etching of n-type silicon wafers in a 5.5% aqueous HF solution (25 ml HF, 200 ml deionized (DI) water and 1 ml NCW-1001 surfactant) (Rong et al. 2008). The anodization process was performed in the absence of light at room temperature in a Teflon cell and using a computer-controlled source meter. Prior to membrane preparation, the silicon wafer was treated to avoid the formation of a parasitic layer by etching at 40 mA/cm^2 for 30 s, and immersing it in a 1 M NaOH solution (Sciacca et al. 2011). Then, the sample was cleaned with DI water and ethanol three times, and dried under a stream of N_2 gas. The pre-treated wafer was etched in two consecutive steps, at 40 mA/cm^2 for 100 s generating a first porous layer, and then at three different current densities in order to fabricate different pore diameters of the second layer. Current intensities used were: 11.3 mA/cm^2 for 175 s, 14.3 mA/cm^2 for 140 s and 19.8 mA/cm^2 for 100 s. The bilayered architecture was used to increase the stability of the free-standing pSi membrane. The membrane was detached from the silicon substrate by applying a series of three 1.28 s high current pulses of 187 mA/cm^2 with 50% duty cycle. This pSi membrane was thoroughly rinsed with ethanol and flipped over before being transferred to a gold slide.

2.4. Functionalization of the pSi membrane

The functionalization of the pSi with an immobilized antibody was performed as shown in Scheme 1 (steps 4-6). First, the freshly etched pSi membrane was thermally hydrosilylated with neat undecylenic acid at 150 °C for 12 h under an Ar gas stream. The functionalized surface was then rinsed with ethanol in order to remove any excess of undecylenic acid from the surface. The carboxyl-terminated membrane was mounted in a Teflon cell prior to antibody immobilization. Firstly, this involved incubation with 5 mM EDC and 5 mM NHS in 0.1M MES buffer, pH 5, at room temperature for 30 min to form a succinimidyl ester group. Subsequently, 25 µg/mL monoclonal anti-MS2 in 0.1 M PBS, pH 7.4, was added and incubated overnight at 4 ºC. The remaining ester groups were deactivated with 0.1 M ethanolamine in PBS for 45 min. After each step, the pSi membrane was thoroughly rinsed with PBS. A negative control immunosensor was prepared under the same conditions but using a non-specific antibody instead.

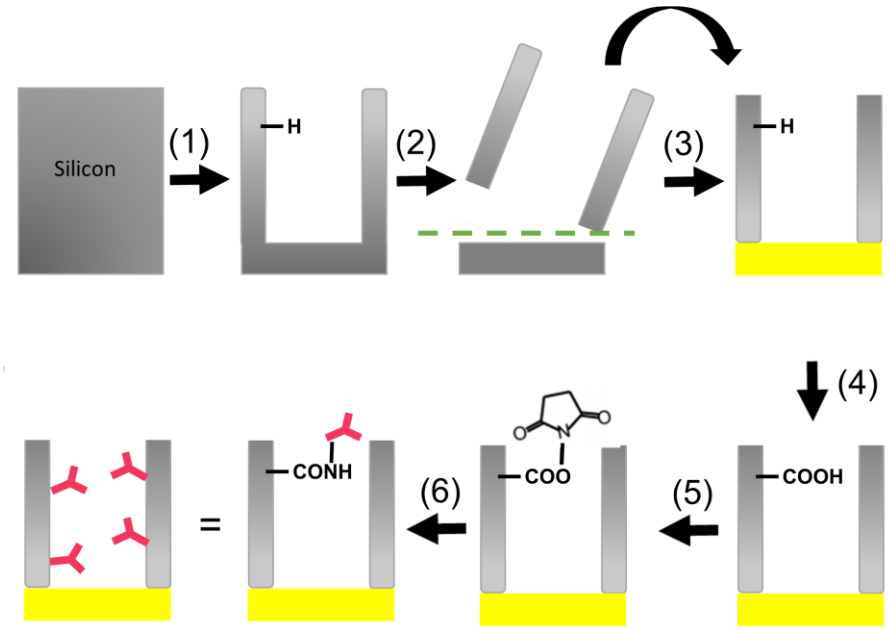

Scheme 1. Schematic of the fabrication of the pSi membrane-based immunosensor, involving the following steps: (1) electrochemical anodization, (2) pSi film detachment by

electropolishing, (3) flipping over the membrane and transfer to gold slide (4) thermal hydrosilylation with undecylenic acid, (5) EDC/NHS activation and (6) antibody immobilization.

2.5. Electrochemical detection

MS2 bacteriophage solutions were incubated on the biosensor surface for 30 min in a wide range of concentrations, from 1 to 10^{10} pfu/mL. After each incubation step, the biosensor was copiously washed with PBS. Electrochemical measurements were performed in a solution of 2 mM $K_4[Fe(CN)_6]$ and 2 mM $K_3[Fe(CN)_6]$ in 0.1 M PBS. DPV was employed as the electrochemical detection technique to measure the oxidation current of the electroactive species. Differential pulse voltammograms were obtained by scanning the potential from -0.3 to 0.8 V. To verify that the current changes were caused only by the specific interaction between MS2 and the anti-MS2 antibody, electrochemical analysis of an immunosensor with a non-specific antibody was evaluated under identical conditions. Each assay was performed in triplicate.

2.6. Experiments involving river water

Untreated water from the Myponga reservoir (Myponga, South Australia) was diluted 10 times in PBS and spiked with MS2 bacteriophage to obtain solutions from 1 to 10^{10} pfu/mL. Electrochemical measurements were carried out in 2 mM $K_4[Fe(CN)_6]$ and 2 mM $K_3[Fe(CN)_6]$ in 0.1 M PBS. Each assay was performed in triplicate.

3. Results and Discussion

3.1. Morphological characterization of the pSi membrane

Anodically etched n-type pSi films contain well-defined nanochannels with high density. The nanochannel diameter can be controlled from 20 nm to 120 nm by changing the current density during anodization. The sensing mechanism applied in this work is based on the blockage of the nanochannels and therefore, nanochannel diameter should allow binding of MS2 bacteriophage (20 nm) (Blanch et al. 2002; Golmohammadi et al. 1993) to the antibody (10 nm of average size) (Reth 2013) immobilized in the pSi membrane.

PSi membranes were fabricated as bilayered structures. The first layer, in direct contact with the transducer in the biosensor design, was etched at 40 mA/cm^2 for all the membranes in order to gain mechanical stability. The second layer, exposed to the solution in the biosensor design, was etched at different current intensities to study the effect of the nanochannel diameter on the biosensor sensitivity. To do so, three different current densities were used. Figure 1 a-c show the top view of the pSi membranes fabricated at: (a) 11.3 mA/cm^2, (b) 14.3 mA/cm^2 and (c) 19.8 mA/cm^2, resulting in membranes with average nanochannel diameters of 40± 15 nm, 57± 17 nm and 85 ± 23 nm, respectively. Figure d shows the bilayered architecture of the membrane fabricated at 19.8 mA/cm^2 with a total thickness of ~ 4.5 µm.

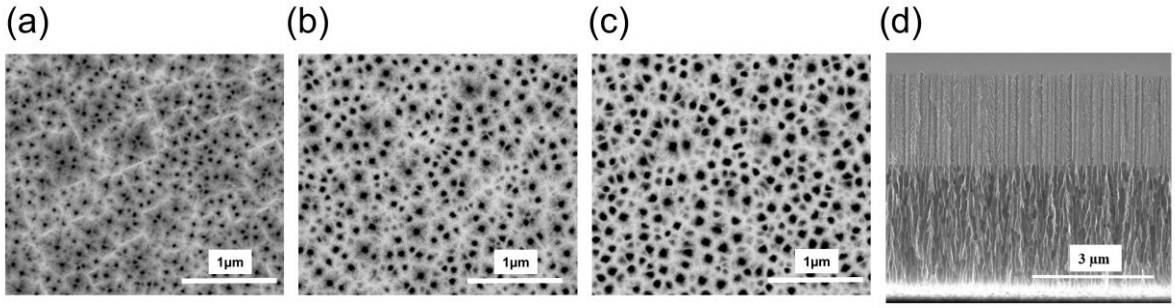

Figure 1. SEM micrographs of top view membranes fabricated at (a) 11.3 mA/cm^2, (b) 14.3 mA/cm^2 and (c) 19.8 mA/cm^2, and of the cross-sectional view of the membrane fabricated at 19.8 mA/cm^2 (d).

3.2. FT-IR characterization of the pSi membrane

All surface modification steps described in section 2.4 were characterized by FT-IR in reflectance mode as shown in Figure 2.

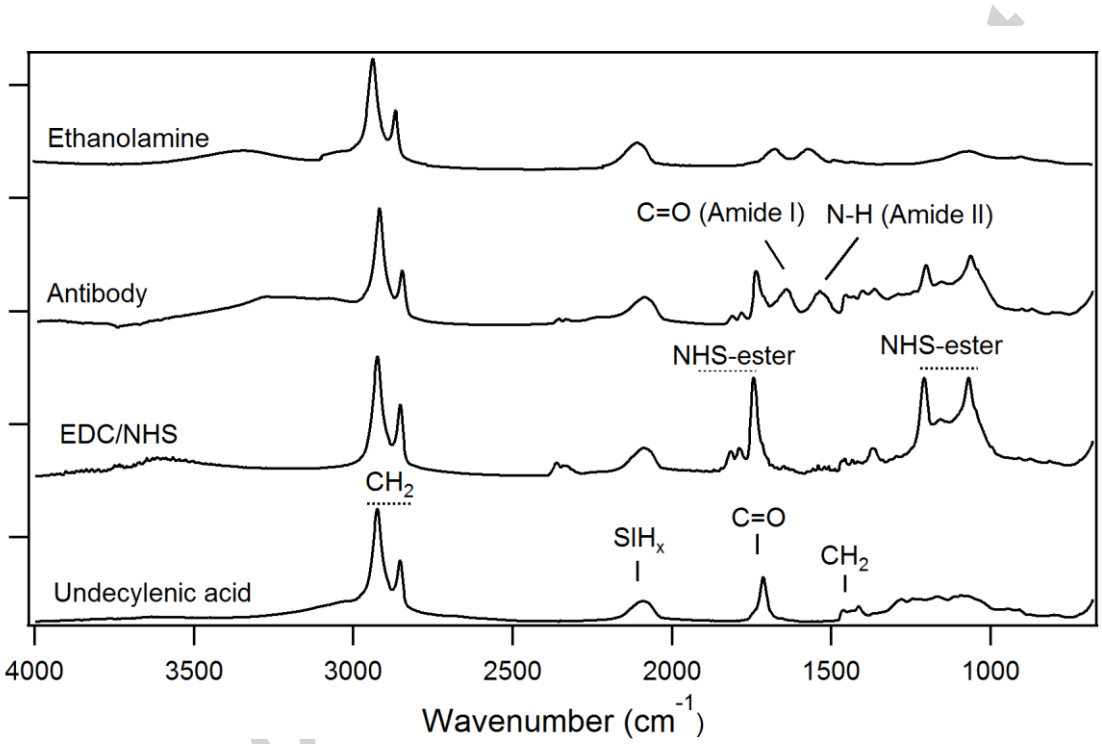

Figure 2. Reflectance mode FT-IR spectra of the pSi membrane after (1) thermal hydrosilylation, (2) EDC/NHS activation, (3) antibody immobilization and (4) quenching with ethanolamine.

Spectrum 1 in Figure 2 exhibits bands at 1714, 2890 and 2940 cm^{-1} corresponding to the νC=O stretching vibrational mode of the carboxylic acid and the stretching νCH_2

stretching vibrational mode of aliphatic C-H bonds, respectively. These vibrations provide evidence for the successful grafting of undecylenic acid to the channel walls. The carboxyl-terminated layer was activated with EDC/NHS forming a succinimidyl ester-terminated surface. This reaction is confirmed in the Spectrum 2 by the prominent triplet of bands in the range of C=O vibrations at 1740, 1785 and 1815 cm^{-1}, which correspond to the antisymmetric and symmetric νC=O mode of the carbonyl groups, and to the succinimidyl moiety, respectively (Sam et al. 2009). The two broad bands in Spectrum 3 at 1650 and 1550 cm^{-1}, correspond to the peptide νC=O stretch (amide I) and peptide νN-H bend (amide II) respectively, demonstrating the successful immobilization of the antibody. Finally, the absence of the characteristic triplet band in Spectrum 4 confirms that the unreacted NHS-ester groups were quenched with ethanolamine.

3.3. Electrochemical characterization of the pSi membrane modification

Modification of the pSi membrane was also electrochemically characterized to confirm the immobilization of the MS2 antibody in the nananochanels. Current intensity before and after antibody immobilization was measured by DPV (Figure S1 in Supplementary data). As expected, the current intensity decreased due to the partial blockage caused by the covalent binding of the antibody in the channels. The magnitude of the current intensity demonstrated that the nanochannels were only partially blocked, allowing the monitoring of further blockage caused upon MS2 bacteriophage binding.

3.4. Electrochemical detection of MS2 bacteriophage

The sensing principle for the detection of MS2 bacteriophage is shown in Scheme 2. When MS2 bacteriophage is captured by the immobilized antibody this causes the partial blockage of nanochannels and, therefore, hinders the diffusion towards the gold surface of the electroactive species added in solution. Blockage is measured by the decrease in the intensity current produced by the oxidation of $K_4[Fe(CN)_6]$.

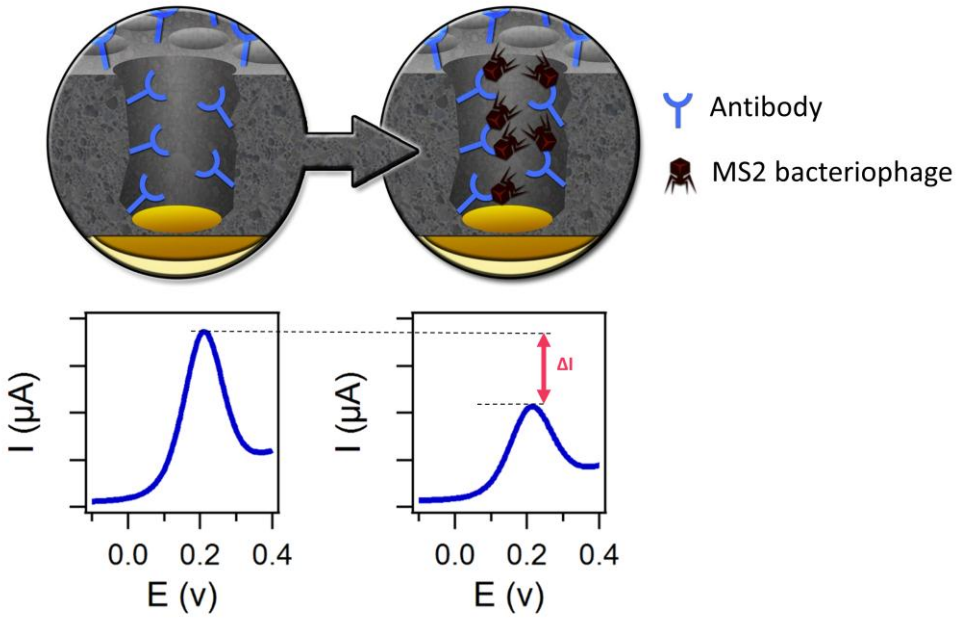

Scheme 2. Sensing principle of the pSi immunosensor for the label-free detection of MS2 bacteriophage and the corresponding DPV traces (a) prior and (b) after bacteriophage interaction.

Figure 3a-c show the DPV traces obtained after incubating the immunosensors prepared with pSi membranes with average nanochannel diameters of (a) 85 nm, (b) 57 nm and (c) 40 nm for a range of MS2 bacteriophage concentrations, from 1 to 10^{10} pfu/mL, spiked in buffer. As expected, the oxidation current decreased as the bacteriophage concentration increased for all immunosensors regardless the nanochannel diameter of the

pSi membrane. However, whilst the immunosensors with the smaller nanochannel diameters (Figure 3b and Figure 3c) showed saturation after incubating with 10^8 pfu/mL MS2, no saturation was seen for the immunosensor with the largest nanochannel diameter in the tested concentration range. To allow comparison of the MS2 antibodies modified immunosensors and the negative controls, modified with non-specific antibodies, all current intensity values were normalized as follows: $\Delta I = (I_0 - I_i)/I_0$, where ΔI was the normalized current change and I_0 and I_i were the current intensity values measured prior and after bacteriophage interaction. In Figure 3d ΔI was plotted as a function of Log [MS2] in order to determine the sensitivity of the immunosensors as the slope of the linear curve fit (fitting parameters provided in Table S2, Supplementary data). These curves show that the sensitivity of the non-specific immunosensors (square symbols) was negligible compared to the sensitivity of the MS2 immunosensors (round symbols), confirming that current changes observed (Figure 3a-c) were a result of the specific binding interactions between the MS2 antibodies immobilized in the nanochannel and MS2 bacteriophage. The sensitivity decreased while decreasing the diameters; the immunosensor with the largest diameter showing the highest sensitivity. The limit of detection (LOD) was calculated using the equation $3S_a/b$, where S_a is the standard deviation of the y-axis and b is the slope (Ziegel 2004)). This was found to be 6, 10 and 19 pfu/mL for the immunosensors based on pSi membranes with 85, 57 and 40 nm nanochannel diameters, respectively.

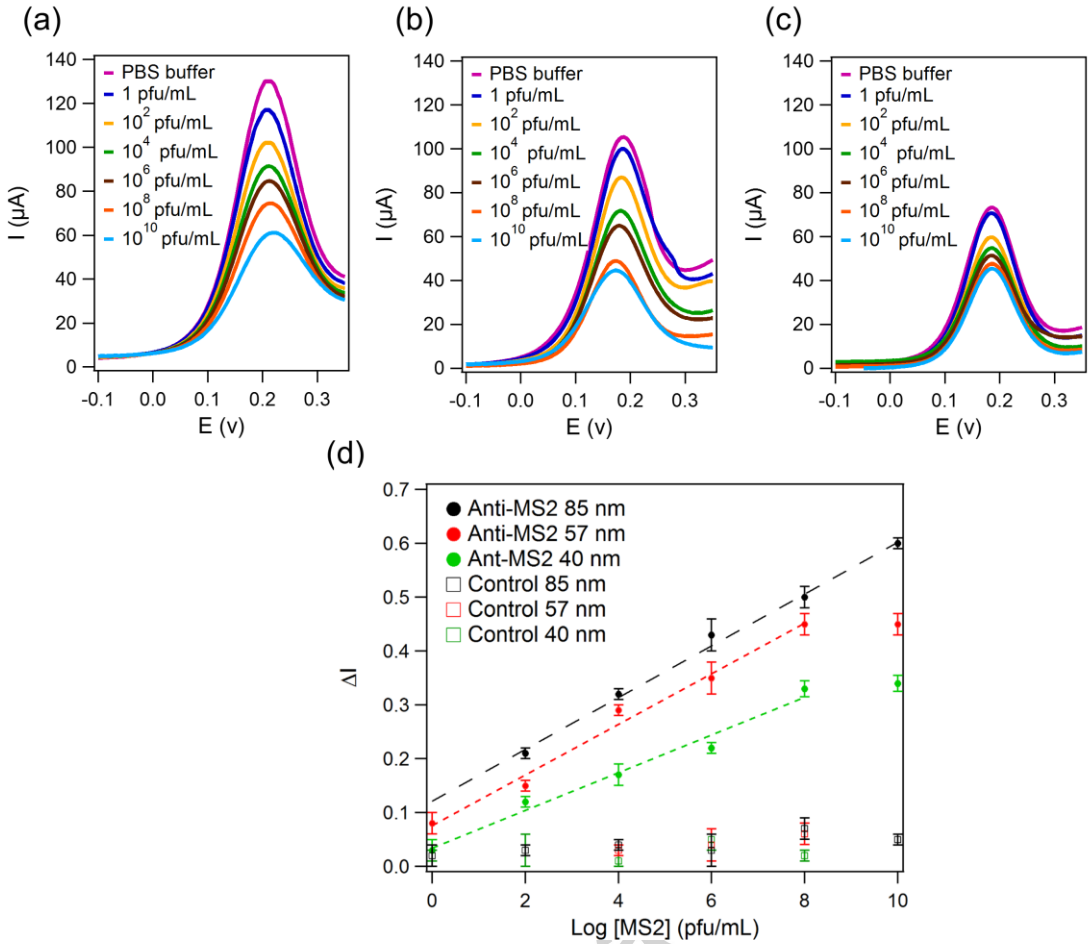

Figure 3. Differential pulse voltammograms (a-c) for increasing concentration of MS2 in PBS for the anti-MS2 antibodies modified immunosensors with membranes of an average diameter of (a) 85 nm, (b) 57 nm and (c) 40 nm, and (d) dose response curves for all immunosensors functionalized with either MS2-specific antibodies or non-specific antibodies (control). Measurements were performed at 0.1 V/s in a 2 mM $K_4[Fe(CN)_6]$ and 2 mM $K_3[Fe(CN)_6]$ solution.

Having successfully optimized the nanochannel diameter (85 nm) of the pSi membrane providing the most sensitive MS2 immunosensor, detection of MS2 bacteriophage in river water samples was attempted as shown in Figure 4.

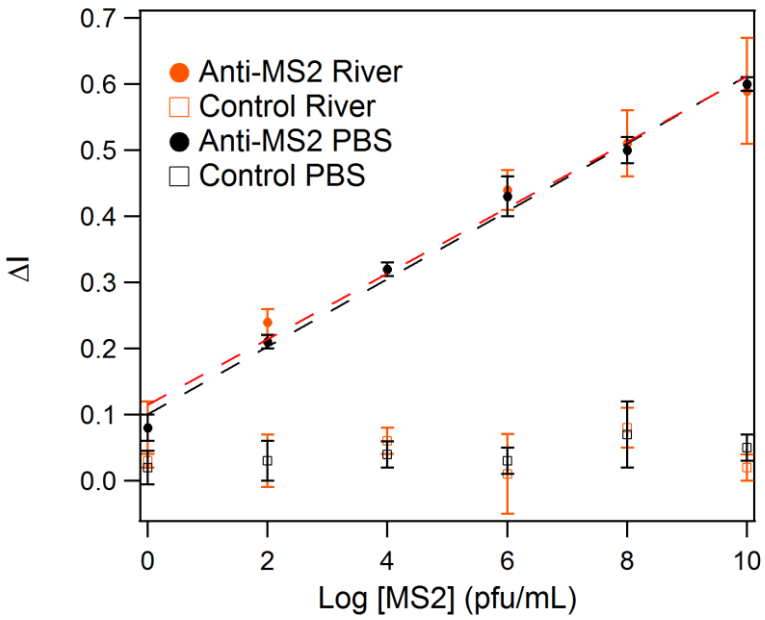

Figure 4. Dose response curves of MS2 bacteriophage for the MS2-specific (circles) and non-specific (squares) immunosensors prepared with a pSi membrane of 85 nm nanochannel diameter in river water (red) and PBS buffer (black).

The percentage of slope deviation between dose response curves in buffer and in river water samples was lower than 3%, indicating the capacity to detect MS2 without significant matrix effects from interfering species that could be present in the river water samples. This could be attributed to the filtering capability of nanoporous materials that exclude the diffusion of species larger than the nanochannel diameter. The LOD, calculated using the results shown in Figure 4 for measurements of MS2 spiked in river water samples, was found to be 17 pfu/mL, which is in the range encountered in real-world applications in wastewater (Keegan et al. 2009) and sewage-impacted wetlands (Li et al. 2012). This excellent LOD for MS2 bacteriophage is comparable to those reported by our group, using electrochemical immunosensors based on carbon nanotube-modified transducers and a sandwich immunoassay (Prieto-Simón et al. 2014), or silicon nanopore arrays and a direct immunoassay (Brodoceanu et al. 2015) (Table S1 in Supplementary data). The main

advantage of our system compared to the sandwich approach is that analysis time is greatly reduced. Furthermore, the analysis cost is reduced by avoiding the use of the immunoreagents. When comparing to the silicon nanopore arrays the fabrication cost is also decreased because our system does not rely in the use of expensive microfabrication processes. Furthermore, our membrane-based sensors showed an excellent stability when stored in PBS buffer over a week (Figure S2 in Supplementary data) with a relative decrease of less than 0.05 in current intensity, being a promising platform for the development of point-of-care portable devices.

Current work in our lab is focused on optimising this pSi platform in order to obtain superior biosensing capabilities towards a wide range of analytes with application in fields ranging from environmental analysis to biomedical diagnostics.

4. Conclusions

We have successfully designed and characterized a label-free ultra-sensitive electrochemical immunosensor based on a nanostructed pSi membrane. Indeed it is the first time that a pSi membrane-based biosensor exploits nanochannel blockage effects to transduce analyte binding.

Our results show that the detection of MS2 bacteriophage can be performed in a simple yet reliable way, with a LOD of 6 pfu/mL in buffer. Moreover, the feasibility to detect MS2 bacteriophage in river water samples is demonstrated. We achieved MS2 bacteriophage detection at levels encountered in wastewater and sewage-impacted wetlands. This excellent analytical performance highlights the potential of this format to be employed in water quality control for real-time measurements.

Finally, the presented label-free electrochemical strategy might open up the possibility to detect a broad range of water- or food-borne analytes, by simply tuning the pSi membrane morphology.

Acknowledgment

We thank for financial support to the Future Industries Institute and International President's Scholarship (IPS) and also acknowledge top-up funding from the National Centre of Excellence in Desalination Australia (NCEDA), as well as, the ARC Linkage (LO130100032).

References

Acquaroli, L.N., Kuchel, T., Voelcker, N.H., 2014. Adv. 4, 34768-34773.
Archer, M., Christophersen, M., Fauchet, P., 2004. Biomed. Microdevices 6, 203-211.
Archer, M., Fauchet, P.M., 2003. physica status solidi (a) 198, 503-507.
Bakker, E., 2004. Anal. Chem. 76, 3285-3298.
Blanch, E.W., Hecht, L., Syme, C.D., Volpetti, V., Lomonossoff, G.P., Nielsen, K., Barron, L.D., 2002. J. Gen. Virol. 83, 2593-2600.
Bonanno, L.M., Kwong, T.C., DeLouise, L.A., 2010. Anal. Chem. 82, 9711-9718.
Brehant, A., Glucina, K., Le Moigne, I., Laine, J.-M., 2010. Desalination 250, 956-960.
Brodoceanu, D., Elnathan, R., Prieto-Simón, B., Delalat, B., Guinan, T., Kroner, E., Voelcker, N.H., Kraus, T., 2015. ACS Appl. Mater. Interfaces 7, 1160-1169.
Campas, M., Garibo, D., Prieto-Simon, B., 2012. Analyst 137, 1055-1067.
Cheng, M.S., Lau, S.H., Chow, V.T., Toh, C.-S., 2011. Environ. Sci. Technol. 45, 6453-6459.
Dancil, K.-P.S., Greiner, D.P., Sailor, M.J., 1999. J. Am. Chem. Soc. 121, 7925-7930.
de la Escosura-Muñiz, A., Chunglok, W., Surareungchai, W., Merkoçi, A., 2013. Biosens. Bioelectron. 40, 24-31.
de la Escosura-Muniz, A., Mekoci, A., 2010. Chem. Commun. 46, 9007-9009.
de la Escosura-Muñiz, A., Merkoçi, A., 2010. Electrochem. Commun. 12, 859-863.
de la Escosura-Muñiz, A., Merkoçi, A., 2011. Small 7, 675-682.
de la Escosura-Muñiz, A., Merkoçi, A., 2012. ACS Nano 6, 7556-7583.
Golmohammadi, R., Valegård, K., Fridborg, K., Liljas, L., 1993. J. Mol. Biol, 234, 620-639.
Grieshaber, D., MacKenzie, R., Voeroes, J., Reimhult, E., 2008. Sensors 8, 1400-1458.
Harraz, F.A., 2014. Sensors and Actuators B: Chemical 202, 897-912.
Holthausen, D., Vasani, R.B., McInnes, S.J.P., Ellis, A.V., Voelcker, N.H., 2012. ACS Macro Lett. 1, 919-921.
Jane, A., Dronov, R., Hodges, A., Voelcker, N.H., 2009. Trends in Biotechnology 27, 230-239.
Jenie, S.N.A., Pace, S., Sciacca, B., Brooks, R.D., Plush, S.E., Voelcker, N.H., 2014. ACS Appl. Mater. Interfaces 6, 12012-12021.
Kant, K., Yu, J., Priest, C., Shapter, J.G., Losic, D., 2014. Analyst 139, 1134-1140.
Keegan, A., Monis, P., Jagals, P., 2009. IWA Publishing.
Kilian, K.A., Böcking, T., Gaus, K., Gal, M., Gooding, J.J., 2007. ACS Nano 1, 355-361.
Koh, G., Agarwal, S., Cheow, P.-S., Toh, C.-S., 2007. Electrochim. Acta 53, 803-810.
Krismastuti, F.S.H., Pace, S., Voelcker, N.H., 2014. Adv. Funct. Mater. 24, 3639-3650.
Li, Y., Sturm, A., Cunningham, P., Bury, N., 2012. BMC Evolutionary Biology 12, 137.
Lugo, J., Ocampo, M., Kirk, A., Plant, D., Fauchet, P., 2007. J. New Mat. Electr. Sys. 10, 113.
Nguyen, B.T.T., Koh, G., Hui, S.L., Chua, A.J.S., Ng, M.M.L., Toh, C.S., 2009. Anal. Chem. 81, 7226-7234.
Nguyen, B.T.T., Peh, A.E.K., Chee, C.Y.L., Fink, K., Chow, V.T.K., Ng, M.M.L., Toh, C.-S., 2012. Bioelectrochemistry 88, 15-21.
Orosco, M.M., Pacholski, C., Miskelly, G.M., Sailor, M.J., 2006. Adv. Mater. 18, 1393-1396.
Peh, A.E.K., Li, S.F.Y., 2013. Biosens. Bioelectron. 42, 391-396.
Prieto-Simón, B., Bandaru, N.M., Saint, C., Voelcker, N.H., 2014. Biosens. Bioelectron.
Rai, V., Deng, J., Toh, C.-S., 2012a. Talanta 98, 112-117.
Rai, V., Hapuarachchi, H.C., Ng, L.C., Soh, S.H., Leo, Y.S., Toh, C.-S., 2012b. PLoS ONE 7, e42346.

Reddy, R.R.K., Basu, I., Bhattacharya, E., Chadha, A., 2003. Current Applied Physics 3, 155-161.
Reth, M., 2013. Nature immunology 14, 765-767.
Rong, G., Ryckman, J.D., Mernaugh, R.L., Weiss, S.M., 2008. Appl. Phys. Lett. 93, 161109-161109-161103.
Sam, S., Touahir, L., Salvador Andresa, J., Allongue, P., Chazalviel, J.N., Gouget-Laemmel, A.C., Henry de Villeneuve, C., Moraillon, A., Ozanam, F., Gabouze, N., Djebbar, S., 2009. Langmuir 26, 809-814.
Sciacca, B., Secret, E., Pace, S., Gonzalez, P., Geobaldo, F., Quignard, F., Cunin, F., 2011. Journal of Materials Chemistry 21, 2294-2302.
Song, M.-J., Yun, D.-H., Min, N.-K., Hong, S.-I., 2007. J. Biosci. Bioeng. 103, 32-37.
Szili, E.J., Jane, A., Low, S.P., Sweetman, M., Macardle, P., Kumar, S., Smart, R.S.C., Voelcker, N.H., 2011. Sensors and Actuators B: Chemical 160, 341-348.
Urmann, K., Walter, J.-G., Scheper, T., Segal, E., 2015. Anal. Chem. 87, 1999-2006.
Vamvakaki, V., Chaniotakis, N.A., 2008. Electroanalysis 20, 1845.
Vestergaard, M., #039, delanji, Kerman, K., Tamiya, E., 2007. Sensors 7, 3442-3458.
Voelcker, N.H., Alfonso, I., Ghadiri, M.R., 2008. ChemBioChem 9, 1776-1786.
Yogeswaran, U., Kumar, S.A.C., Shen-Ming, Nanotechnology Science and Technology : Nanostructured Materials for Electrochemical Biosensors. Nova Science Publishers, Incorporated, New York, NY, USA.
Zhang, J., Wu, Y., Zhang, B., Li, M., Jia, S., Jiang, S., Zhou, H., Zhang, Y., Zhang, C., Turner, A.P.F., 2012. Anal. Lett. 45, 986-992.
Ziegel, E.R., 2004. Technometrics 46, 498-499.

Highlights

Label-free ultrasensitive porous silicon nanochannel array

Immunosensor based on nanochannel blockage using differential pulse voltammetry

MS2 was detected at levels found in wastewater and sewage-impacted environments